Published in final edited form as:
Nat Cell Biol. 2013 October ; 15(10): 1176–1185. doi:10.1038/ncb2829.

Riquiqui and Minibrain, new regulators of the Hippo pathway downstream of Dachsous

Joffrey Degoutin[1,2], **Claire C. Milton**[1,2,3], **Eefang Yu**[1,2], **Marla Tipping**[4], **Floris Bosveld**[5], **Yohanns Bellaiche**[5], **Alexey Veraksa**[4], and **Kieran F. Harvey**[1,2,3,6]

[1]Cell Growth and Proliferation Laboratory, Peter MacCallum Cancer Centre, 7 St Andrews Place, East Melbourne, Victoria, Australia, 3002

[2]Sir Peter MacCallum Department of Oncology, University of Melbourne, Parkville, Victoria, Australia, 3010

[3]Department of Pathology, University of Melbourne, Parkville, Victoria, Australia, 3010

[4]Department of Biology, University of Massachusetts Boston, Boston, MA, USA 02125

[5]Polarity, Division and Morphogenesis Team, Institut Curie, CNRS UMR 3215, INSERM U934, 26 Rue d'Ulm, 75248 Paris Cedex 05, France

Abstract

The atypical cadherins, Fat (Ft) and Dachsous (Ds) control tissue growth via the Salvador-Warts-Hippo (SWH) pathway, and also regulate planar cell polarity (PCP), proximo-distal (PD) patterning and morphogenesis. Ft and Ds engage in reciprocal signalling as both proteins can serve as receptor and ligand for each other. The intracellular domains (ICD) of Ft and Ds regulate activity of the key SWH pathway transcriptional co-activator protein Yorkie (Yki). Signalling from the Ft ICD is well characterized and controls tissue growth by regulating abundance of the Ykirepressive kinase Warts (Wts). Here we describe two new regulators of the SWH pathway that function downstream of the Ds ICD: the WD40 domain protein Riquiqui (Riq) and the DYRK-family kinase Minibrain (Mnb). Ds physically interacts with Riq, which forms a complex with both Mnb and Wts. Riq and Mnb promote Ykidependent tissue growth by stimulating phosphorylation-dependent inhibition of Wts. Thus, we describe a new branch of the SWH pathway that promotes tissue growth downstream of Ds.

INTRODUCTION

Organ size is controlled by many factors including morphogens and nutrients. The Salvador-Warts-Hippo (SWH) pathway has been theorized to control organ size based on the fact that

[6]Corresponding author, kieran.harvey@petermac.org, Telephone: 61 3 9656 1291, Fax: 61 3 9656 1411.

CONTRIBUTIONS

J.D. and C.C.M. performed *Drosophila* genetic experiments. J.D. and E.Y. carried out biochemistry and molecular biology experiments. M.T. and A.V. performed affinity pruification followed by mass spectrometry. F.B. and Y.B. analyzed Dachs localization in the pupal notum. J.D. and K.F.H. designed experiments, analyzed data and wrote the manuscript.

COMPETING FINANCIAL INTERESTS

The authors declare no competing financial interests.

modulation of pathway activity influences the size of both *D. melanogaster* and murine organs[1-4]. Deregulation of SWH pathway activity has also been linked to carcinogenesis in humans[1]. The best-defined receptor for the SWH pathway is the large atypical cadherin, Ft[5-9], which is activated by binding to its ligand, the related cadherin Ds[10, 11]. Both Ft and Ds possess several extracellular cadherin repeats and cytoplasmic tails that mediate intracellular signalling events[4, 12, 13]. Several studies show that Ds not only acts as a ligand for Ft but also functions as a receptor that signals via its intracellular domain (ICD) to regulate PCP and SWH pathway activity[10, 14, 15]. For example, the Ds ICD is required for *D. melanogaster* imaginal disc cells to derepress Yki activity in response to ectopic *ds* expression[10]. In addition, in a *ds* mutant background, *ds ICD* overexpression activates Yki and causes tissue overgrowth in a cell-autonomous fashion[14]. Ft is likely to act as a ligand for Ds because Ds is partially required for overexpression of the Ft extracellular domain (ECD) to trigger Yki hyperactivation[14]. Therefore, Ds can both promote Yki activity cell-autonomously, and repress Yki activity non-cell autonomously by signalling via Ft.

The mechanism by which Ft mediates cell-autonomous repression of Yki is relatively well-defined[4, 12, 16]. Upon binding to Ds on neighbouring cells, Ft controls imaginal disc growth via downstream proteins that include the atypical myosin Dachs[9], the LIM-domain protein Zyxin[17] and the palmitoyltransferase Approximated[18]. These proteins influence activity of the SWH pathway core kinase cassette, by regulating abundance of the Wts kinase[9, 17]. Wts in turn represses tissue growth by phosphorylating and inhibiting the Yorkie (Yki) transcriptional co-activator protein[19]. Ft also controls stability and subcellular localization of Expanded (Ex)[5-7], another upstream regulator of the SWH pathway, while the Four-jointed (Fj) kinase regulates the interaction between the ECDs of Ft and Ds[20-22].

In contrast to signalling from the Ft ICD to the SWH pathway, signalling events downstream of the Ds ICD are poorly defined. Ds ICD regulates morphogenesis by polarizing Dachs[13], and has been proposed to activate Yki by sequestering SWH pathway proteins at the apical membrane[14], but this idea has not been interrogated. Here we describe the identification of a membrane-to-nucleus Ds signalling pathway that promotes Yki activity by repressing Wts. Unlike the Ft branch of the SWH pathway, Ds-mediated regulation of Wts and Yki occurs independent of Dachs. By contrast, Ds promotes Yki activity by signalling via the WD40 domain protein Riq and the DYRK family kinase Mnb to induce phosphorylation-mediated repression of Wts.

RESULTS

Riquiqui, a newly-identified Dachsous-interacting protein

The atypical cadherins Ds and Ft act as a ligand-receptor pair to control tissue growth, PCP and PD patterning[10, 14, 15, 23-25]. The ECDs of these proteins form physical complexes and initiate signalling events between neighbouring cells[21, 22]. Signalling downstream of the Ft ICD has begun to be elucidated in recent years[4, 12, 16]. Ds controls morphogenesis by influencing the apical membrane polarity of Dachs[13], but the mechanism by which it controls Yki activity and tissue growth is poorly understood. To address this knowledge gap we attempted to identify proteins that signal downstream of the Ds ICD. Using affinity purification in *Drosophila melanogaster* S2 cells followed by mass spectrometry[26], we

identified proteins that interact with the Ds ICD. An abundant Ds-interacting protein was the uncharacterized protein CG14614, hereafter referred to as Riquiqui (Riq) referring to its small size phenotype, as described below. Riq is a 343 amino acid protein and contains a WD40 domain predicted to mediate protein-protein interactions. Riq homologues are present throughout the animal kingdom and in plants, and are highly conserved; *D. melanogaster* Riq and its human homologue (known as DCAF7 or Han11) are 85% identical and 91% similar. The zebrafish Riq homologue Wdr68 has been implicated in craniofacial development[27], but Riq function has not been studied *in vivo* in other organisms. To confirm Riq as a Ds-interacting protein we performed immunoprecipitation experiments using transfected S2 cell lysates. As shown in Fig. 1a, a robust physical interaction was detected between Riq and the Ds ICD.

Riquiqui regulates tissue growth

In conjunction with Ft, Ds controls tissue growth by modulating activity of the SWH pathway[10, 11]. In order to investigate a potential role for Riq in tissue growth, we modulated its expression in the developing eye, wing and leg by generating UASinducible *riq* transgenes, and with the use of independent *riq* RNAi transgenes that target different regions of the *riq* gene. A slight decrease in adult eye size was observed when *UAS-riq RNAi* was expressed using *GMR-Gal4*, compared to control eyes expressing a *UAS-LacZ* transgene (Fig. 1b). In the converse experiment, a modest increase in eye size was observed when *riq* was overexpressed using *GMR-Gal4*. Alterations in eye size are often accompanied by changes in interommatidial cell (IOC) number in pupal eye discs when assessed 44 hours after puparium formation (APF). When *riq* was overexpressed we observed an increase in IOC number compared to control (Fig. 1c).

We further explored a role for Riq in tissue growth by modulating its expression in developing wings using *rotund-Gal4* (*rn-Gal4*). RNAi-mediated depletion of Riq caused a 21% or 32% decrease in wing size depending on the RNAi line used (Fig. 1d). Conversely, *riq* overexpression caused an 11% increase in wing size. We confirmed that the reduced wing size observed when *riq* RNAi was expressed was due to Riq depletion by showing expression of a *riq* transgene rescued the reduction in wing size (Fig. 1d). Further, expression of *riq* RNAi lines substantially reduced expression of endogenous Riq protein in developing wing imaginal discs, as determined using an antibody against the human Riq homologue, DCAF7 (Supplementary Fig. S1a). Riq knockdown was also confirmed by real time PCR; *riq* transcript was depleted by almost 50% in wing discs expressing *UAS-riq* RNAi under control of *hedgehog (hh)-Gal4* (Supplementary Fig. S1b). We also assessed a role for Riq in leg growth by driving expression of *riq* RNAi or the *riq* transgene using *hh-Gal4*. Legs expressing *riq* RNAi were 9% shorter, while *riq* overexpression increased leg length by 7% (Fig. 1e). Collectively, these data suggest that Riq regulates IOC number in the eye, and the size of wings, eyes and legs.

The Minibrain kinase forms a physical complex with Riquiqui and is functionally related

The human Riq homologue, DCAF7 has been shown to physically complex with the human Dyrk1a kinase (homologous to *D. melanogaster* Mnb)[28]. Given the high degree of conservation of Riq, we investigated the possibility that Riq and Mnb physically and

functionally interact in *D. melanogaster*. Initially, we tested whether Riq and Mnb physically interact by performing co-immunoprecipitation experiments on S2 cell lysates expressing epitope-tagged versions of Mnb and Riq. As shown in Fig. 2a, a robust physical association was observed between Riq and Mnb.

Subsequently, we investigated a potential role for Mnb in leg and wing growth. To characterize the role of Mnb in leg development, we measured the size of legs from flies expressing a *mnb* RNAi transgene or flies that were hemizygous for a mutant allele of *mnb* called mnb^{1} that has been shown to express approximately 60% to 70% less Mnb protein[29]. In each case, the length of the tarsal segments of these flies was 7% smaller than control flies (Fig. 2b). To investigate a role for Mnb in wing growth we expressed *mnb* RNAi with *rn-Gal4* and found that adult wings were significantly smaller (Fig. 2c), mirroring our earlier observation with Riq. Importantly, this reduction in size was observed using two independent *mnb* RNAi transgenes directed against independent regions of the *mnb* gene, thus ruling out off-target effects (Fig. 2c). Consistent with a role for Mnb as a growth-promoting protein, *rn-Gal4* driven *mnb* overexpression led to a 15% increase in wing size. A role for *mnb* in wing growth was further substantiated by assessing wing size in flies that were hemizygous for mnb^{1}; these flies possessed wings that were 19% smaller than wild-type flies (Fig. 2c'). These findings show that Mnb, like Riq, is required for normal wing growth.

To begin to assess whether Mnb and Riq control wing growth together we used *rn-Gal4* to simultaneously overexpress Riq, and deplete Mnb by RNAi. Mnb depletion completely suppressed Riq's ability to promote wing overgrowth as these wings were undergrown and were of similar size to wings expressing the *mnb RNAi* alone (Fig. 2c). Collectively, our biochemical and genetic data support a model whereby Riq and Mnb function together to promote tissue growth.

Riquiqui and Mnb regulate activity of the SWH pathway oncoprotein Yorkie

Ds has been postulated to control SWH pathway activity by acting both as a receptor and ligand for Ft[10, 14, 23]. Based on our above data, we hypothesized that Riq and Mnb control tissue growth downstream of the Ds ICD by modulating SWH pathway activity. To address this hypothesis we modulated expression of Mnb and Riq and assessed Yki activity using *lacZ* enhancer traps in the *ex, thread* (*th* or *Diap1*) and *bantam* (*ban*) genes. Both *riq* and *mnb* overexpression caused Yki activity to increase, as indicated by increases in *ex-lacZ, th-lacZ* or *ban-lacZ* (Fig. 3a-d). Consistent with these findings, RNAi-mediated depletion of either Riq or Mnb led to reduced Yki activity, as determined by *th-lacZ* (Fig. 3e,f). Collectively, these experiments suggest that Riq and Mnb regulate tissue growth by controlling SWH pathway activity.

Riquiqui and Minibrain repress the SWH pathway by phosphorylating and inhibiting the Warts kinase

Ft controls SWH pathway activity by polarizing the localization of Dachs at the apical membrane of epithelial cells[9], while Ds polarizes Dachs to regulate morphogenesis[13]. However we found no evidence that Ds controls tissue growth via Dachs, as modulating the

expression of either Riq or Mnb had no influence on Dachs levels or localization in wing imaginal discs, and these proteins appeared to control wing size in parallel to each other (Supplementary Fig. S2). To further investigate the mechanism by which Mnb and Riq regulate the SWH pathway we used a biochemical approach. Given that Mnb is a kinase, we hypothesized that it phosphorylates a component(s) of the SWH pathway. To test this notion we co-expressed Mnb with different SWH pathway proteins in S2 cells and assessed their mobility by SDS-PAGE. When co-expressed with Mnb the mobility of Wts was decreased (Fig. 4a), while Hpo and Sav were unaffected (data not shown). Mnb's ability to alter Wts mobility was potentiated by Riq because when S2 cells co-expressed Wts, Mnb and Riq, Wts mobility was further decreased (Fig. 4a). Riq alone had no impact on Wts mobility showing that it requires exogenous Mnb to influence Wts mobility. Mnb's ability to influence Wts mobility was also observed when these proteins were co-expressed with Sav and Hpo, which are known to regulate Wts phosphorylation (Supplementary Fig. S3a).

To investigate whether the observed change in Wts mobility was the result of phosphorylation, we generated a kinase-dead version of Mnb by mutating the ATP-binding site (Mnb K386R). Co-expression of Mnb K386R with Wts failed to modify Wts mobility in the presence or absence of Riq (Fig. 4b), showing that Mnb requires its kinase activity to modulate Wts mobility. For several reasons, we also investigated whether Homeodomain-interacting protein kinase (Hipk) could alter the mobility of Wts; Hipk is the closest Mnb homologue in *D. melanogaster*; Hipk's human orthologue (HIPK2) can also physically interact with the human Riq orthologue (DCAF7)[30]; and we and others have recently shown that Hipk regulates tissue growth via the SWH pathway[31, 32]. However, in contrast to Mnb, Hipk had no effect on Wts mobility, suggesting that it does not phosphorylate Wts (Supplementary Fig. S3b).

We then explored which region of Wts was phosphorylated by Mnb, by expressing three portions of Wts protein with or without Mnb. Only Wts1, representing amino acids 1-318, showed a clear mobility change in the presence of Mnb (Fig. 4c'). To determine whether Mnb could indeed phosphorylate this portion of Wts we performed *in vitro* kinase assays using recombinant GST-Wts1 as a substrate. Immunoprecipitations were performed on lysates from untransfected cells or cells expressing either Mnb or Mnb K386R. After incubation in kinase buffer supplemented with γ^{32}P-ATP Mnb, but not Mnb K386R, displayed strong autophosphorylation confirming that the K386R mutation renders Mnb inactive (Fig. 4c"). Mnb stimulated strong phosphorylation of GST-Wts1, whereas Mnb K386R did not. These data show that Mnb indeed phosphorylates Wts, and does so by phosphorylating one or more residues between amino acids 1-318.

Given that Mnb could phosphorylate Wts *in vitro* we sought to determine whether Mnb and/or Riq physically interact with Wts. Immunoprecipitations were performed on lysates obtained from S2 cells transfected with different combinations of epitope-tagged versions of Mnb, Riq and Wts. Initially, we found that Wts and Mnb could form a physical complex in S2 cells (Fig. 5a). We then investigated whether Riq and Wts could interact by immunoprecipitating Riq with an antibody directed against human DCAF7, which we previously found to cross-react with Riq in imaginal discs (Supplementary Fig. S1a). We were able to detect a weak but consistent physical interaction between Riq and Wts (Fig.

5a'). We also co-transfected Wts, Mnb and Riq together in S2 cells and detected physical interactions between each protein (Fig. 5a"). These experiments suggest that Mnb, Wts and Riq can form a complex that allows Mnb to phosphorylate Wts.

Next, we investigated the functional consequence of Riq/Mnb-dependent phosphorylation of Wts. Based on our observations that Riq and Mnb normally promote tissue growth and Yki activity, we hypothesized that Riq and Mnb repress Wts activity. To interrogate this hypothesis we assayed Wts activity in the presence or absence of Mnb by assessing Yki phosphorylation. Wts stimulates phosphorylation of Yki on at least three residues, with S168 being the major site[33, 34]. Co-expression of Mnb with Yki did not influence basal phosphorylation of Yki at S168, as detected by a phospho-Yki-S168 antibody (Fig. 5b). In the presence of Sav, Wts and Hpo, Yki was strongly phosphorylated at S168; when quantified across three independent experiments, a 3.7-fold increase was observed (Fig. 5b'). When Mnb was also expressed together with Sav, Wts and Hpo a strong reduction of Yki-S168 phosphorylation was observed; in this setting Yki-S168 phosphorylation was similar to that observed in cells expressing Yki alone (Fig. 5b,b'). These data are consistent with the idea that Riq and Mnb promote tissue growth by repressing Wts, thus derepressing Yki.

Dachsous requires Riquiqui and Minibrain to activate Yorkie

To determine whether Riq and Mnb function downstream of the Ds ICD to regulate the ability of Wts to limit Yki activity, we performed a series of experiments in developing *D. melanogaster* tissues. We first overexpressed *ds* in the posterior compartment of wing imaginal discs using *hh-Gal4* and found that Yki activity, as assessed by *ex-lacZ*, was strongly increased especially in the wing pouch (Fig. 6a). Interestingly, and as reported previously, non-*ds* overexpressing cells at the AP border also showed a strong increase in *ex-lacZ* (Fig. 6a")[14]. We hypothesized that depletion of Riq or Mnb would suppress the ability of *ds* overexpression to induce Yki activity without affecting non-cell autonomous Yki elevation in anterior wing disc cells. Our experiments showed that indeed *ex-lacZ* levels in the posterior wing disc were greatly reduced when either Riq or Mnb were depleted by RNAi, but that Yki hyperactivation in anterior cells near the AP boundary was unaffected (Fig. 6b-c"). Mnb and Riq depletion also affected Ds-induced effects on tissue morphology: *ds* overexpression caused wing disc convolution and this was suppressed by Mnb or Riq depletion (X-Z sections in Fig. 6a-c). Suppression of Ds-induced Yki activation was not caused by a reduced Ds expression as depletion of neither Mnb nor Riq, affected Ds levels (Supplementary Fig. S4).

Consistent with the idea that signalling downstream of the Ds ICD regulates Yki activity upon Ds-Ft binding, expression of the Ft ECD (*ft*Δ*ICD*) can hyperactivate Yki in a Ds-dependent fashion[14]. In order to determine if Ds-dependent activation of Yki requires Riq and Mnb, we overexpressed *ft*Δ*ICD* in the posterior compartment of the wing and assessed Yki activity in the absence or presence of *riq* RNAi. *ft*Δ*ICD* expression strongly increased *ex-lacZ* and caused substantial overgrowth and folding of the posterior wing disc (Fig. 6d). RNAi mediated depletion of Riq in *ft*Δ*ICD*-expressing tissues partially suppressed both of these phenotypes (Fig. 6e). To further characterize this effect, we used the *32B-Gal4* driver

to express *ft*Δ*ICD* with or without *riq* RNAi throughout wing imaginal discs. Depletion of Riq in *ft*Δ*ICD*expressing discs caused an 11% decrease in *ex* and a 31% decrease in *Diap1*, as assessed by RT-PCR (Fig. 6f). These data support the idea that, in response to Ft-Ds binding, the Ds ICD promotes Yki-dependent tissue growth by signalling via Riq and Mnb to alleviate Wts-dependent repression of Yki (Fig. 7).

DISCUSSION

The related cadherins, Ft and Ds, control tissue growth by regulating SWH pathway activity[5-7, 9-11], and also control PCP and PD patterning[12, 23]. Intriguingly, Ft and Ds regulate SWH pathway activity by engaging in reciprocal signalling as a ligand-receptor pair. Signalling downstream of Ft is reasonably well defined, but signalling downstream of Ds has remained relatively obscure until the discovery of a membrane-to-nucleus signalling pathway controlling SWH pathway activity downstream of the Ds ICD, described here. Our genetic and biochemical data implies that, upon ligation of the Fat and Ds ECDs, the WD40 domain protein Riq complexes with the Ds ICD and the Mnb and Wts kinases. Riq promotes Mnb-dependent phosphorylation and inhibition of Wts, and thereby promotes Yki-dependent tissue growth.

Therefore, Ds-Ft ligation induces two seemingly opposing growth-regulatory events: Ds activates Ft, which represses Yki by modulating Dachs [10, 11]; while Ft signals via Ds, Riq and Mnb to activate Yki. At first glance it seems counterintuitive that Ft-Ds binding would both promote, and repress Yki-dependent tissue growth but raises several interesting possibilities. One option is that the timing of signalling from both the Ds ICD and the Ft ICD is different and varies throughout the cell cycle. For example, Ds ICD might deliver a pulse of Yki activity to induce transcriptional events associated with tissue growth. Subsequently, to ensure that Yki activity does not perdure and cause tissue overgrowth, it could be repressed by signalling from Ft ICD. Alternatively, Ds ICD or Ft ICD signalling might predominate over the other in different regions of imaginal discs or at different stages of development, to regulate Yki. How such regulation could occur is unclear, but could possibly: 1) stem from polarized activity of Ft and Ds that occurs in cells of growing imaginal discs in response to graded expression of Ds and Fj[21, 22]; 2) occur if the influence of signalling downstream of Ft ICD or Ds ICD on Wts activity was quantitatively different; 3) result from non-uniform activity of additional proteins that mediate Ft and Ds signalling. Alternatively, repression of Yki by the Ft ICD, and activation by the Ds ICD, could quantitatively oppose each other and serve to set a fine threshold of Yki activity that is highly sensitive to regulation by other branches of the SWH pathway such as the Kibra-Expanded-Merlin proteins[35-38], the Hpo activating kinase Tao-1[39, 40], or apicobasal polarity proteins[41-44]. In future studies it will be important to define the spatiotemporal activity profile of Ft ICD and Ds ICD signalling and the relative influence of the Ds and Ft branches of the SWH pathway on tissue growth.

Given that Ft and Ds also engage in bi-directional signaling to control PCP[15] and PD patterning[24], it will be important to determine whether Riq and Mnb control these processes downstream of the Ds ICD. Finally, given the emergence of the SWH pathway as an important regulator of different human tumours[1], the present study raises the possibility that

the human orthologues of Riq (DCAF7) and Mnb (Dyrk1a and Dyrk1b) could function as oncogenes.

METHODS

Drosophila melanogaster stocks

Riquiqui knockdown was performed using two RNAi lines: *UAS-riqRi1* (KK 107076) from Vienna Drosophila RNAi Center (VDRC) and *UAS-riqRi2* (14614R-1) from the Japanese National Institute of Genetic (NIG). Minibrain knockdown was performed using two RNAi lines: *UAS-mnbRi1* (KK 107066) and *UAS-mnbRi2* (GD 28628) both from VDRC. The *riq* overexpression line was engineered by injection of a *pUAST-riq* construct cloned by PCR from the CG14614 cDNA obtained from DGRC (clone LD15927). *UAS-mnb* was provided by K. Yu. Other stocks were: *UAS-Ds*, *UAS-EYFP*, *ex-lacZ; hh-Gal4*, *ban-lacZ; hh-Gal4*, *en-Gal4; th-LacZ*, *UAS-dachs*, *UAS-dachs RNAi*, *salm-Gal4*, *rn-Gal4*, *hh-Gal4* and *GMR-Gal4*. The mnb^1 allele was provided by F. Tejedor. Clones of *UAS-riqRi1* and *UAS-mnbRi1* were obtained by crossing UAS lines with the *actin-Gal4* flip out stock: *hsflp; actin>CD2>Gal4, UAS-GFP*.

Quantification of wing size and leg length

Wing area from female or male (as specified) flies reared at 25°C was quantified using Adobe Photoshop. The tarsal segment (comprising T1 to 5) of the right back leg of female adult flies was quantified using Image J. The mean and S.E.M values of wing area or tarsal length were determined using GraphPad Prism. To assess statistical significance, each genotype was compared using one-way ANOVA followed by a Bonferroni post-test. P values <0.05 were considered significant.

Immunostaining

We used the following primary antibodies: mouse anti-β-galactosidase (Sigma), rat anti-Cubitus-Interruptus, mouse anti-Disc-large (both from Developmental Studies Hybridoma Bank), rabbit anti-DCAF7 (Novus Biologicals), rat anti-Dachs (gift from D. Strutt) and rat anti-Dachsous (gift from M Simon). Secondary antibodies (anti-rat, anti-mouse and anti-rabbit) were from Invitrogen. Third instar larval imaginal discs and pupal eye discs (44 hours APF) were stained as in[45, 46].

Plasmids

The Ds ICD (DsΔECD) was amplified by PCR from pUAST-DsΔECD[47] and cloned into the pAc5.1 and GS-TAP vectors[26]. The Riq open reading frame was PCR-amplified from DGRC clone LD15927, epitope-tagged and cloned into pAc5.1. pMT-Mnb. HA was obtained from I.Edery[48]. pMT-Mnb K386R.HA was generated by site-directed mutagenesis. pAc5.1-Wts.V5 and pAc5.1-Yki.HA were from D. Pan[19]. pAc5.1-Hpo.FLAG and pAc5.1-Sav.myc were from N. Tapon[49]. Portions of Wts were amplified by PCR and cloned into pAc5.1. pAc5.1-myc.HipK was described in[31]. Wts1 was cloned into pGEX-4T1 for bacterial expression.

Cell culture, transfection and western blot analysis

S2 cells were cultured in Schneider's Drosophila medium (Gibco) supplemented with 10% FBS (Gibco) and 1% Penicillin/streptomycin (Gibco). Cells were transfected with the indicated plasmids using the Effectene transfection reagent (Qiagen). $CuSo_4$ was added to culture media at a final concentration of 0.35mM when using pMT based plasmids. After 48 hours, cells were lysed using a RIPA buffer (10 mm NaP_i buffer, pH 7.8, 60 mM NaCl, 1% Triton X-100, 0.5% deoxycholic acid, 0.1% SDS, 10% glycerol, 25 mM β-glycerol phosphate, 50 mM sodium fluoride, 2 mM sodium pyrophosphate, 1 mM sodium orthovanadate, and protease inhibitor Complete, Roche) and subjected to SDS-PAGE then transferred to a PVDF membrane (Millipore). In order to visualize differences in Wts mobility, 3-8% Tris Acetate gels were used (Invitrogen). 4-12% Bis-Tris gels were used for other experiments. Membranes were immunobloted with the following antibodies: rabbit ant-HA, mouse anti-V5, mouse anti-Tubulin (all from Invitrogen), rabbit anti-Phospho-S168-Yorkie (gift from N. Tapon). HRP coupled secondary antibodies were from Dako. Detection was performed using the ECL prime Western Blotting Detection form Amersham. Images were taken using the ChemiDoc MP (Biorad). Quantification of bands was performed with Image J.

Kinase assay

S2 cells were transfected with Mnb or Mnb K386R. Two days after transfection, cells were lysed in DISC lysis buffer [150 mM NaCl, 2 mM EDTA, 1% Triton X-100, 10% glycerol and 20 mM Tris pH 7.5, 10 mM NaF, 2 mM Na pyrophosphate, 5 mM β-glycerophosphate and PhosStop phosphatase inhibitor cocktail (Roche) and Complete Mini protease inhibitor cocktail (Roche)] and immunoprecipitated using anti-HA (Invitrogen). BL-21 bacteria transformed with pGEX-4T1-GST-Wst1 were incubated with 1mM IPTG at 37°C to induce GST-Wts1. Recombinant protein was purified using Glutathione sepharose, and eluted in 50mM Tris-HCl, 10mM Glutathione, 0.05% Triton X-100, pH8. Equivalent amounts of GST-Wts1 were used in each kinase assay. Equivalent amounts of immunoprecipitates were divided into the combinations noted in the figure legend in kinase buffer [50 mM Hepes pH 7.4, 10 mM MgCl2, 1mM DTT, 10% glycerol, 1 mM EDTA, 1 mM EGTA, 100 mM NaCl, 1 mM NaF, 5 mM β-glycerophosphate, 100 μM ATP, PhosStop phosphatase inhibitor cocktail and Complete Mini protease inhibitor cocktail]. 5μCi γ^{32}P-ATP (Perkin Elmer) was added to each sample and incubated at 30°C for 30 minutes as in[50]. The reaction was stopped by the addition of 5X protein loading buffer, boiled at 95°C and subjected to SDS-PAGE. Gels were dried and exposed to a Phosphorimager screen (Molecular Dynamic) and analysed using the Typhoon Trio Phosphorimager and ImageQuant software (GE Healthcare) as in[39].

Quantitative Real Time PCR

RNA was extracted from wing imaginal discs by Trizol (Invitrogen), and used to generate cDNA with Superscript III (Invitrogen). Quantitative PCR reactions were performed on Applied Biosystems Step One Plus software with Fast SYBR Green Master Mix (Applied Biosystems) and primers designed to detect *ex*, *Diap1* and *Actin 5C* mRNA as in[51].

Supplementary Material

Refer to Web version on PubMed Central for supplementary material.

Acknowledgments

We thank J. Lin for expertise with kinase assays and S. Blair, I. Edery, K. Irvine, D. Pan, M. Simon, D. Strutt, N. Tapon, F. Tejedor, K. Yu, the Developmental Studies Hybridoma Bank, the Vienna *Drosophila* RNAi Center, the Australian *Drosophila* Research Support Facility (www.ozdros.com), the National Institute of Genetics and the Bloomington Stock Centre for fly stocks, plasmids and antibodies. K.F.H is a Sylvia and Charles Viertel Senior Medical Research Fellow. This research was supported by a Project Grant from the National Health and Medical Research Council of Australia, and by NIH grants GM097727 and CA156734 and NSF grant 0640700 to A.V. Mass spectrometry was performed at the Taplin Mass Spectrometry Facility, Harvard Medical School.

References

1. Harvey K, Tapon N. The Salvador-Warts-Hippo pathway - an emerging tumour-suppressor network. Nature reviews Cancer. 2007; 7:182–191.
2. Badouel C, Garg A, McNeill H. Herding Hippos: regulating growth in flies and man. Curr Opin Cell Biol. 2009; 21:837–843. [PubMed: 19846288]
3. Halder G, Johnson RL. Hippo signaling: growth control and beyond. Development. 2011; 138:9–22. [PubMed: 21138973]
4. Reddy BV, Irvine KD. The Fat and Warts signaling pathways: new insights into their regulation, mechanism and conservation. Development. 2008; 135:2827–2838. [PubMed: 18697904]
5. Bennett FC, Harvey KF. Fat cadherin modulates organ size in Drosophila via the Salvador/Warts/Hippo signaling pathway. Curr Biol. 2006; 16:2101–2110. [PubMed: 17045801]
6. Willecke M, et al. The fat cadherin acts through the hippo tumor-suppressor pathway to regulate tissue size. Curr Biol. 2006; 16:2090–2100. [PubMed: 16996265]
7. Silva E, Tsatskis Y, Gardano L, Tapon N, McNeill H. The tumorsuppressor gene fat controls tissue growth upstream of expanded in the hippo signaling pathway. Curr Biol. 2006; 16:2081–2089. [PubMed: 16996266]
8. Tyler DM, Baker NE. Expanded and fat regulate growth and differentiation in the Drosophila eye through multiple signaling pathways. Dev Biol. 2007; 305:187–201. [PubMed: 17359963]
9. Cho E, et al. Delineation of a Fat tumor suppressor pathway. Nat Genet. 2006; 38:1142–1150. [PubMed: 16980976]
10. Willecke M, Hamaratoglu F, Sansores-Garcia L, Tao C, Halder G. Boundaries of Dachsous Cadherin activity modulate the Hippo signaling pathway to induce cell proliferation. Proc Natl Acad Sci U S A. 2008; 105:14897–14902. [PubMed: 18809931]
11. Rogulja D, Rauskolb C, Irvine KD. Morphogen control of wing growth through the Fat signaling pathway. Dev Cell. 2008; 15:309–321. [PubMed: 18694569]
12. Sopko R, McNeill H. The skinny on Fat: an enormous cadherin that regulates cell adhesion, tissue growth, and planar cell polarity. Curr Opin Cell Biol. 2009; 21:717–723. [PubMed: 19679459]
13. Bosveld F, et al. Mechanical control of morphogenesis by Fat/Dachsous/Four-jointed planar cell polarity pathway. Science. 2012; 336:724–727. [PubMed: 22499807]
14. Matakatsu H, Blair SS. Separating planar cell polarity and Hippo pathway activities of the protocadherins Fat and Dachsous. Development. 2012; 139:1498–1508. [PubMed: 22399682]
15. Casal J, Lawrence PA, Struhl G. Two separate molecular systems, Dachsous/Fat and Starry night/Frizzled, act independently to confer planar cell polarity. Development. 2006; 133:4561–4572. [PubMed: 17075008]
16. Grusche FA, Richardson HE, Harvey KF. Upstream regulation of the hippo size control pathway. Curr Biol. 2010; 20:R574–582. [PubMed: 20619814]
17. Rauskolb C, Pan G, Reddy BV, Oh H, Irvine KD. Zyxin links fat signaling to the hippo pathway. PLoS Biol. 2011; 9:e1000624. [PubMed: 21666802]

18. Matakatsu H, Blair SS. The DHHC palmitoyltransferase approximated regulates Fat signaling and Dachs localization and activity. Curr Biol. 2008; 18:1390–1395. [PubMed: 18804377]
19. Huang J, Wu S, Barrera J, Matthews K, Pan D. The Hippo signaling pathway coordinately regulates cell proliferation and apoptosis by inactivating Yorkie, the Drosophila Homolog of YAP. Cell. 2005; 122:421–434. [PubMed: 16096061]
20. Ishikawa HO, Takeuchi H, Haltiwanger RS, Irvine KD. Four-jointed is a Golgi kinase that phosphorylates a subset of cadherin domains. Science. 2008; 321:401–404. [PubMed: 18635802]
21. Simon MA, Xu A, Ishikawa HO, Irvine KD. Modulation of Fat:Dachsous Binding by the Cadherin Domain Kinase Four-Jointed. Curr Biol. 2010
22. Brittle AL, Repiso A, Casal J, Lawrence PA, Strutt D. Four-Jointed Modulates Growth and Planar Polarity by Reducing the Affinity of Dachsous for Fat. Curr Biol. 2010
23. Lawrence PA, Struhl G, Casal J. Do the protocadherins Fat and Dachsous link up to determine both planar cell polarity and the dimensions of organs? Nat Cell Biol. 2008; 10:1379–1382. [PubMed: 19043429]
24. Clark HF, et al. Dachsous encodes a member of the cadherin superfamily that controls imaginal disc morphogenesis in Drosophila. Genes Dev. 1995; 9:1530–1542. [PubMed: 7601355]
25. Thomas C, Strutt D. The roles of the cadherins Fat and Dachsous in planar polarity specification in Drosophila. Developmental dynamics : an official publication of the American Association of Anatomists. 2012; 241:27–39. [PubMed: 21919123]
26. Kyriakakis P, Tipping M, Abed L, Veraksa A. Tandem affinity purification in Drosophila: the advantages of the GS-TAP system. Fly (Austin). 2008; 2:229–235. [PubMed: 18719405]
27. Nissen RM, Amsterdam A, Hopkins N. A zebrafish screen for craniofacial mutants identifies wdr68 as a highly conserved gene required for endothelin-1 expression. BMC developmental biology. 2006; 6:28. [PubMed: 16759393]
28. Skurat AV, Dietrich AD. Phosphorylation of Ser640 in muscle glycogen synthase by DYRK family protein kinases. J Biol Chem. 2004; 279:2490–2498. [PubMed: 14593110]
29. Tejedor F, et al. minibrain: a new protein kinase family involved in postembryonic neurogenesis in Drosophila. Neuron. 1995; 14:287–301. [PubMed: 7857639]
30. Ritterhoff S, et al. The WD40-repeat protein Han11 functions as a scaffold protein to control HIPK2 and MEKK1 kinase functions. EMBO J. 2010; 29:3750–3761. [PubMed: 20940704]
31. Poon CL, Zhang X, Lin JI, Manning SA, Harvey KF. Homeodomain-interacting protein kinase regulates hippo pathway-dependent tissue growth. Curr Biol. 2012; 22:1587–1594. [PubMed: 22840515]
32. Chen J, Verheyen EM. Homeodomain-interacting protein kinase regulates yorkie activity to promote tissue growth. Curr Biol. 2012; 22:1582–1586. [PubMed: 22840522]
33. Oh H, Irvine KD. In vivo regulation of Yorkie phosphorylation and localization. Development. 2008; 135:1081–1088. [PubMed: 18256197]
34. Dong J, et al. Elucidation of a universal size-control mechanism in Drosophila and mammals. Cell. 2007; 130:1120–1133. [PubMed: 17889654]
35. Hamaratoglu F, et al. The tumour-suppressor genes NF2/Merlin and Expanded act through Hippo signalling to regulate cell proliferation and apoptosis. Nat Cell Biol. 2006; 8:27–36. [PubMed: 16341207]
36. Genevet A, Wehr MC, Brain R, Thompson BJ, Tapon N. Kibra Is a Regulator of the Salvador/Warts/Hippo Signaling Network. Dev Cell. 2010; 18:300–308. [PubMed: 20159599]
37. Baumgartner R, Poernbacher I, Buser N, Hafen E, Stocker H. The WW Domain Protein Kibra Acts Upstream of Hippo in Drosophila. Dev Cell. 2010; 18:309–316. [PubMed: 20159600]
38. Yu J, et al. Kibra Functions as a Tumor Suppressor Protein that Regulates Hippo Signaling in Conjunction with Merlin and Expanded. Dev Cell. 2010; 18:288–299. [PubMed: 20159598]
39. Poon CL, Lin JI, Zhang X, Harvey KF. The Sterile 20-like Kinase Tao-1 Controls Tissue Growth by Regulating the Salvador-Warts-Hippo Pathway. Dev Cell. 2011; 21:896–906. [PubMed: 22075148]

40. Boggiano JC, Vanderzalm PJ, Fehon RG. Tao-1 Phosphorylates Hippo/MST Kinases to Regulate the Hippo-Salvador-Warts Tumor Suppressor Pathway. Dev Cell. 2011; 21:888–895. [PubMed: 22075147]
41. Grzeschik NA, Parsons LM, Allott ML, Harvey KF, Richardson HE. Lgl, aPKC, and Crumbs regulate the Salvador/Warts/Hippo pathway through two distinct mechanisms. Curr Biol. 2010; 20:573–581. [PubMed: 20362447]
42. Robinson BS, Huang J, Hong Y, Moberg KH. Crumbs regulates Salvador/Warts/Hippo signaling in Drosophila via the FERM-domain protein expanded. Curr Biol. 2010; 20:582–590. [PubMed: 20362445]
43. Ling C, et al. The apical transmembrane protein Crumbs functions as a tumor suppressor that regulates Hippo signaling by binding to Expanded. Proc Natl Acad Sci U S A. 2010; 107:10532–10537. [PubMed: 20498073]
44. Chen CL, et al. The apical-basal cell polarity determinant Crumbs regulates Hippo signaling in Drosophila. Proc Natl Acad Sci U S A. 2010; 107:15810–15815. [PubMed: 20798049]
45. Milton CC, Zhang X, Albanese NO, Harvey KF. Differential requirement of Salvador-Warts-Hippo pathway members for organ size control in Drosophila melanogaster. Development. 2010; 137:735–743. [PubMed: 20110315]
46. Harvey KF, Pfleger CM, Hariharan IK. The Drosophila Mst ortholog, hippo, restricts growth and cell proliferation and promotes apoptosis. Cell. 2003; 114:457–467. [PubMed: 12941274]
47. Matakatsu H, Blair SS. Separating the adhesive and signaling functions of the Fat and Dachsous protocadherins. Development. 2006; 133:2315–2324. [PubMed: 16687445]
48. Chiu JC, Ko HW, Edery I. NEMO/NLK phosphorylates PERIOD to initiate a time-delay phosphorylation circuit that sets circadian clock speed. Cell. 2011; 145:357–370. [PubMed: 21514639]
49. Pantalacci S, Tapon N, Leopold P. The Salvador partner Hippo promotes apoptosis and cell-cycle exit in Drosophila. Nat Cell Biol. 2003; 5:921–927. [PubMed: 14502295]
50. Callus BA, Verhagen AM, Vaux DL. Association of mammalian sterile twenty kinases, Mst1 and Mst2, with hSalvador via C-terminal coiled-coil domains, leads to its stabilization and phosphorylation. FEBS J. 2006; 273:4264–4276. [PubMed: 16930133]
51. Harvey KF, et al. FOXO-regulated transcription restricts overgrowth of Tsc mutant organs. J Cell Biol. 2008; 180:691–696. [PubMed: 18299344]

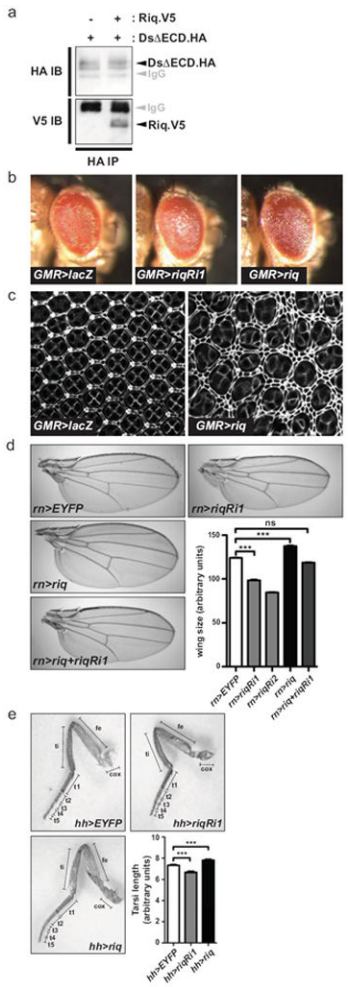

Figure 1. Riquiqui forms a physical complex with Dachsous and controls tissue growth

(a) Lysates from S2 cells transfected with DsΔECD.HA, alone or in combination with Riq.V5, were immunoprecipitated with anti-HA antibodies. Western blots were performed using anti-HA and anti-V5 antibodies to reveal Ds and Riq, respectively. (b) Lateral views of adult female eyes (anterior is to the right) expressing *UAS-lacZ*, *UAS-riqRi1* or *UAS-riq* under the control of *GMR-Gal4*. (c) Eyes 44 hours APF expressing *UAS-lacZ* or *UAS-riq* under the control of *GMR-Gal4* that have been stained with anti-Discs-large antibody. (d) Representative images of wings from adult female flies expressing *UAS-EYFP*, *UAS-riqRi1*, *UAS-riqRi2*, *UAS-riq* or *UAS-riqRi1* concomitantly with *UAS-riq* under the control of *rn-Gal4*. Wing size was quantified for each genotype (n=20 for each). (e) Right rear legs from adult female flies expressing *UAS-EYFP*, *UAS-riqRi1* or *UAS-riq* under the control of *hh-Gal4*. Legend of leg segments is as follows, coxa (cox), femur (fe), tibia (ti), tarsal segments 1 to 5 (t1, t2, t3, t4, t5). The length of the entire tarsal segment was quantified (n=15 for each genotype). In d and e, data are presented as mean ± SEM, *** = $p<0.001$, ns = non-significant.

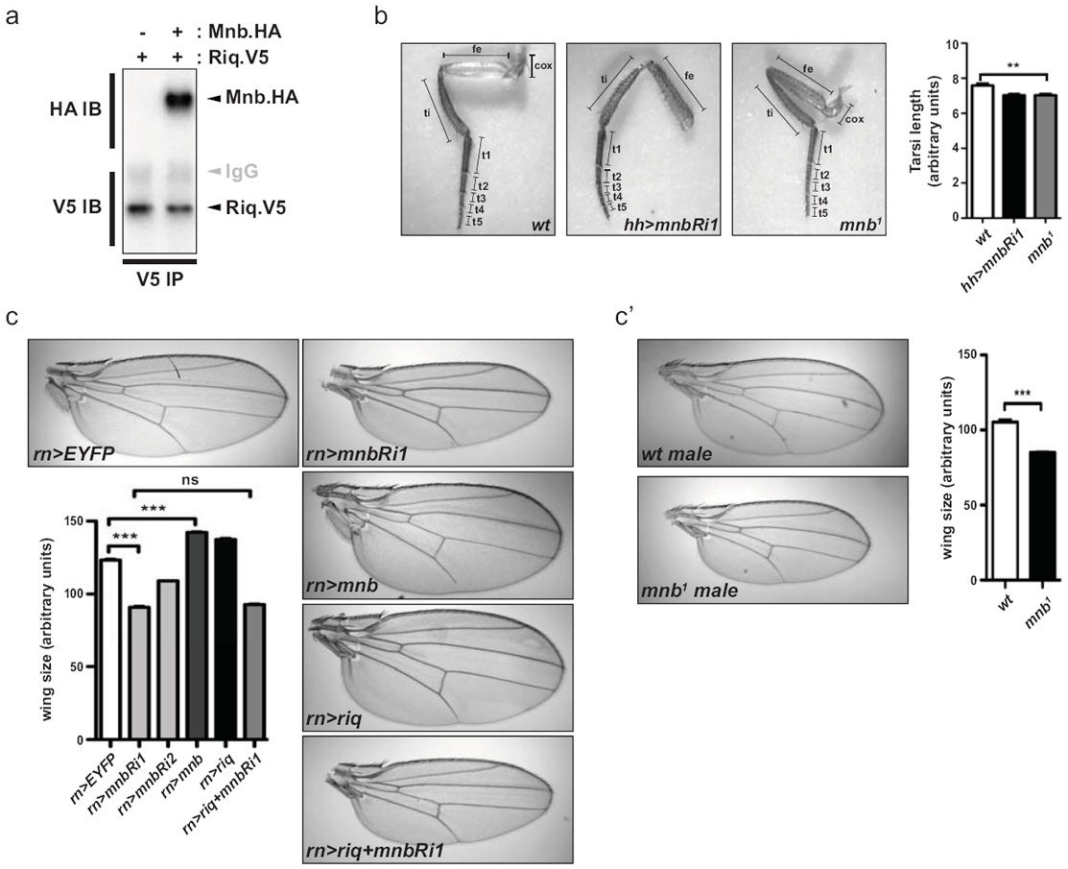

Figure 2. Minibrain interacts with Riquiqui and phenocopies its effect on tissue growth

(a) Lysates from S2 cells transfected with Riq.V5 alone or together with Mnb.HA, were immunoprecipitated with anti-V5 antibodies. Western blots were performed using anti-HA and anti-V5 antibodies to reveal Mnb and Riq, respectively. (b) Images of right rear legs from adult female flies expressing *hh-Gal4* driven *UAS-EYFP* or *UAS-mnbRi1*, or legs from *mnb*^{1} flies. The entire tarsal segment of individual legs was quantified (n=15 for each genotype). Legend of leg segments is as follow, coxa (cox), femur (fe), tibia (ti), tarsal segment 1 to 5 (t1, t2, t3, t4, t5). (c) Wing area from adult female flies expressing *UAS-EYFP* as control, *UAS-mnbRi1*, *UAS-mnbRi2*, *UAS-mnb*, *UAS-riq* or *UAS-mnbRi1* concomitantly with *UAS-riq* under the control of *rn-Gal4.* Representative imagess are shown and wing size was quantified (n=20 for each genotype). (c') Area of adult male wings of *mnb*^{1} mutant flies were quantified and compared to adult male wild-type wings. Representative images are shown. Results from leg and wing quantification (b, c and c') are presented as mean ± SEM, *** = p<0.001, ** = p<0.01.

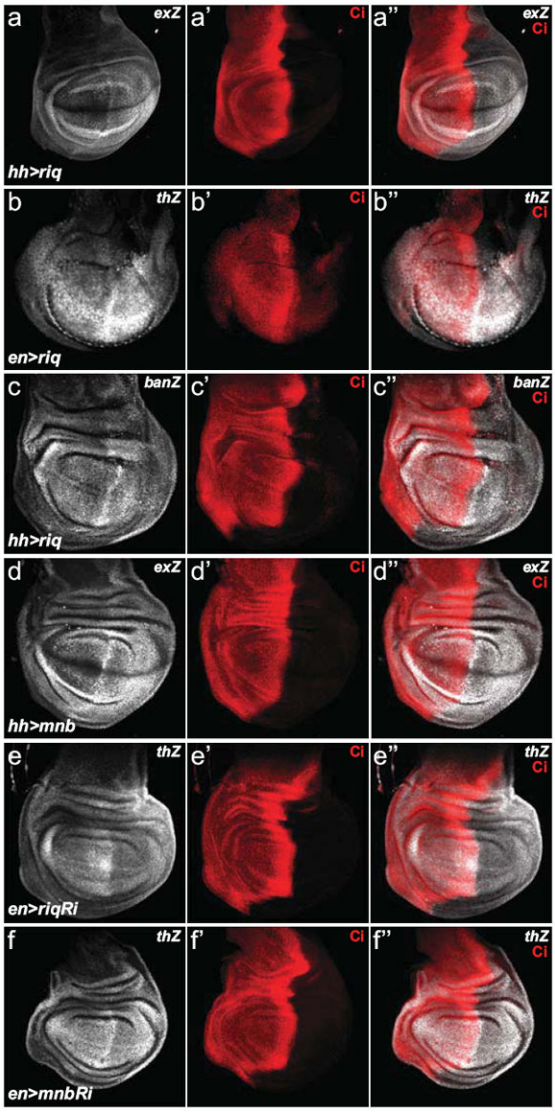

Figure 3. Riquiqui and Minibrain regulate SWH pathway activity

Wing imaginal discs from third instar *D. melanogaster* larvae harbouring the following transgenes: (a) *hh-Gal4, UAS-riq* and *ex-lacZ*; (b) *en-Gal4*, *UAS-riq* and *th-lacZ*; (c) *hh-Gal4, UAS-riq* and *ban-lacZ*; (d) *hh-Gal4, UAS-mnb* and *ex-lacZ*; (e), *en-Gal4*, *UAS-riqRi* and *th-lacZ*; and (f) *en-Gal4*, *UAS-mnbRi* and *th-lacZ*. Yki activity (grey in a-f) was reported by *ex-lacZ* (a and d), *th-lacZ* (b, e and f) or *ban-lacZ* (c). All transgenes were expressed in the posterior compartment of wing imaginal discs; Cubitus interruptus (Ci) expression (red in a'-f') marked the anterior compartment. Merged images are shown in (a"-f").

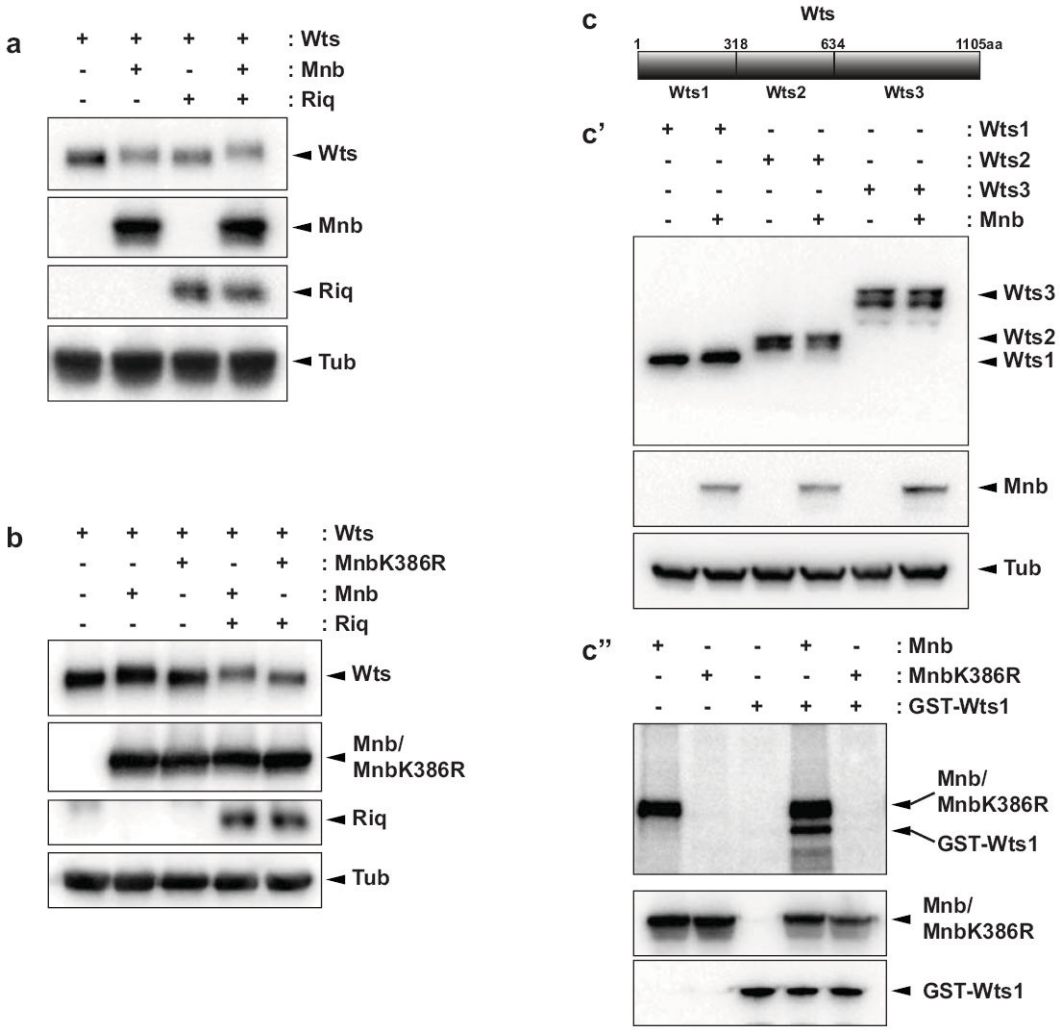

Figure 4. Minibrain phosphorylates Warts

(a and b) Western blot analysis of lysates from S2 cells transfected with the indicated plasmids. Wts and Riq were revealed with anti-V5 and Mnb or Mnb K386R with anti-HA. Tubulin levels were assessed to ensure even protein loading. Note that tubulin displayed no change in mobility. (c) Schematic diagram of the Wts protein and the fragments of Wts (Wts1, Wts2 and Wts3) that were expressed in S2 cells alone or together with Mnb. (c') Western Blot analysis was performed with antibodies to V5 (to reveal Wts), HA (to reveal Mnb) and Tubulin. (c'') A kinase assay performed using recombinant GST-Wts1 as a substrate and either Mnb or Mnb K386R immunoprecipitated from S2 cells. Isolated proteins were incubated alone or together in kinase buffer containing γ^{32}P-ATP and subjected to SDS-PAGE (higher panel). Western blotting was used to detect input proteins (lower panels).

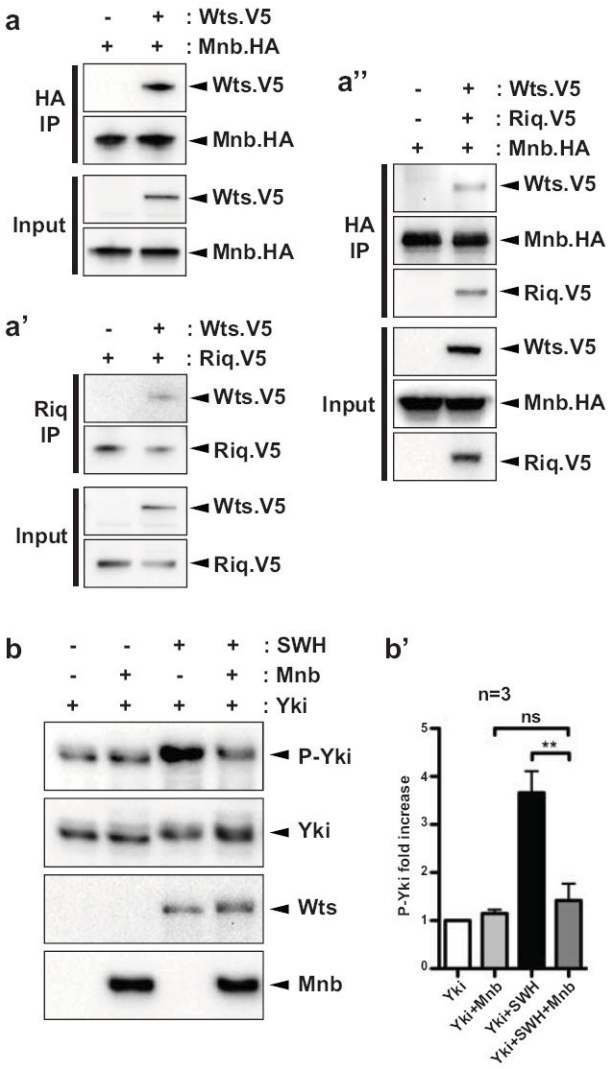

Figure 5. Minibrain and Riquiqui form a physical complex with Warts and inhibit its activity

(a) V5-tagged Wts was expressed alone or together with HA-tagged Mnb or V5-tagged Riq or both (as labeled above the blot) in S2 cells. Cells were lysed and lysates were subjected to immunoprecipitation using the anti-HA antibody or the anti-DCAF7 antibody (homologues of Riq in mammals). Proteins were then revealed using the corresponding antibody. (b) Yki was expressed alone or together with Mnb or a combination of Salvador/Warts/Hippo (SWH) or both in S2 cells. Yorkie phosphorylation was assessed by Western Blot using an anti-PhosphoS168-Yorkie antibody. Fold increase from Phospho-Yki/total Yki over three independent transfections (n=3) has been quantified. **p<0.01, ns = non-significant.

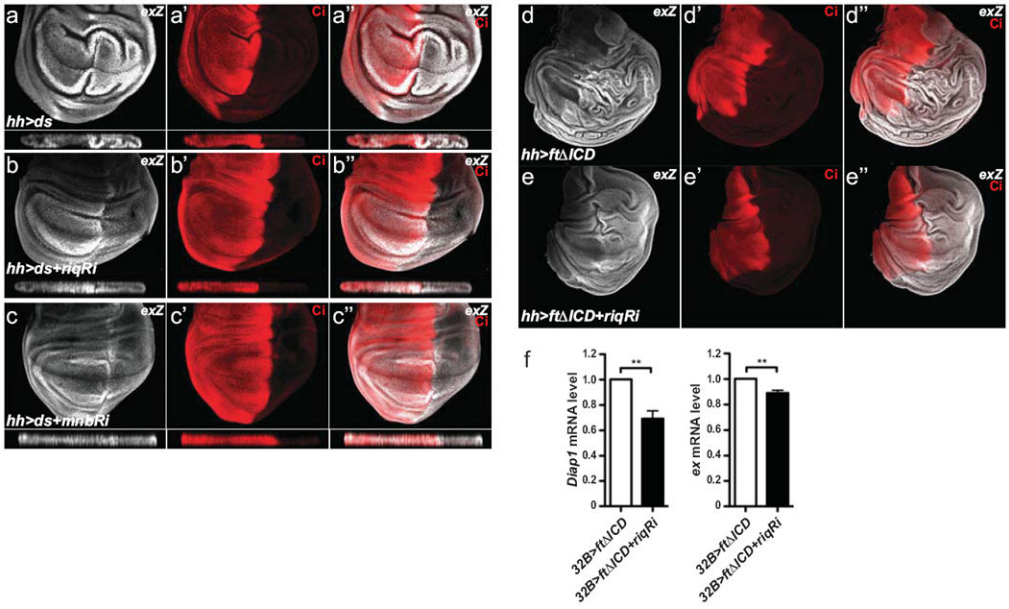

Figure 6. Riquiqui and Minibrain function downstream of Dachsous to promote Yorkie activity

Wing imaginal discs from third instar *D. melanogaster* larvae harbouring the following transgenes: (a) *hh-Gal4, UAS-ds* and *ex-lacZ*; (b) *hh-Gal4, UAS-ds, UAS-riqRi* and *ex-lacZ*; (c) *hh-Gal4, UAS-ds, UAS-mnbRi* and *ex-lacZ*; (d) *hh-Gal4, UAS-ftΔICD* and *ex-lacZ*; (e) *hh-Gal4, UAS-ftΔICD, UAS-riqRi* and *ex-lacZ*. Yki activity was reported by *ex-lacZ* levels (grey in a-e). Cubitus interruptus (Ci) expression (red in a'-e') marked the anterior compartment of wing imaginal discs. Merged images are shown in (a''-e''). X-Z sections through the wing pouch are shown below planar sections of wing discs in a-c". (f) Levels of *ex* mRNA and *Diap1* mRNA relative to the control *actin5C* mRNA, assessed by QRT-PCR, in wing imaginal discs harbouring the following transgenes: *32B-Gal4* and *UAS-ftΔICD*; and *32B-Gal4, UAS-ftΔICD* and *UAS-riqRi*. Data is presented as mean ± SEM, n=3, ** = $p<0.01$.

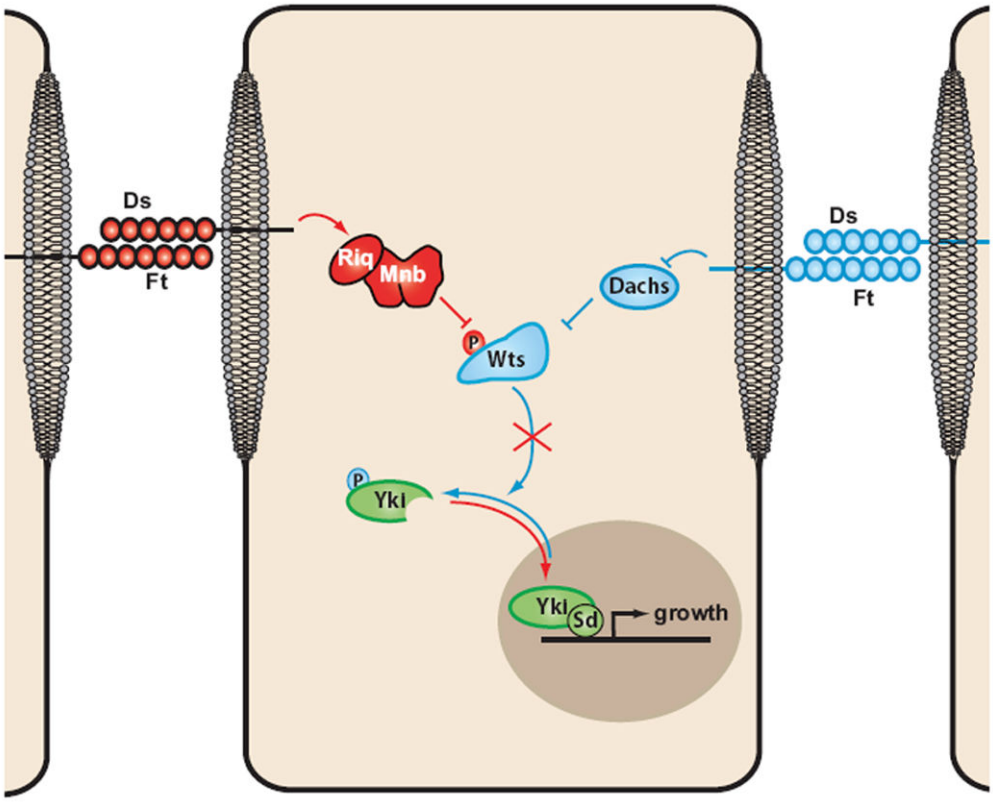

Figure 7. Model of signalling from Dachsous and Fat to the SWH pathway

Signalling from the Ds ICD is represented in red (positively regulating growth) and signalling from the Ft ICD in blue (negatively regulating growth). (Ds: Dachsous, Ft: Fat, Riq: Riquiqui, Mnb: Minibrain, Wts: Warts, Yki: Yorkie, Sd: Scalloped)